DOI: 10.1515/adms-2017-0020

P. Raczyński[1], K. Warnke[2]

[1] Gdansk University of Technology, Faculty of Electronics Telecommunication and Informatics, Gdansk, Poland
[2]CDRiA Pipeline Services Ltd., Warszawa, Poland
pawel.raczynski@cdria.com krzysztof.warnke@cdria.com

ULTRASONIC DIAGNOSTICS OF MAIN PIPELINES

ABSTRACT

The main pipelines, like many engineering structures, are subject to high operational safety standards. The safety of their operation is supervised by various institutions from the operator, including supervisors such as the Office of Technical Inspection. Safe operation requires knowledge of their technical condition and trends. One of the important sources of information on the condition of pipelines is their periodic inspection carried out with so-called smart pigs. As a result of the inspection, the operator expects the following questions to be answered: what is the condition of the pipeline examined; where and what metal losses are occurring in its construction; what are the hazards causing these damages for the safety of the pipeline operation; what is the rate of increase in the size of metal losses in the pipeline wall. This article presents technical solutions and methodology to answer the above questions.

Keywords: *operational safety, smart pigs, ultrasonic scanning, diagnosis, prognosis*

INTRODUCTION

For over 20 years, CDRiA has been active in inspecting oil and fuel pipelines, using proprietary inspection pigs. High-resolution, ultrasonic inline smart tools (brand name KORSONIC) are used for inspecting the condition of a pipeline wall. It involves the use of a traveling robot together with the embossed medium measuring and recording the current parameters of the pipeline construction tested. After inspection, these data are analyzed for the detection and parameterization of existing faults and anomalies such as metal losses, laminations, changes in the geometry of the pipeline wall. Used ultrasonic (UT) smart pigs allow for simultaneous measurement of the wall thickness and detection and precise sizing of defects in the internal geometry of a pipeline.

This paper presents some examples of different applications of the images, including 3D images, offering the presentation of characteristic features of various types of defects detected in pipelines. Additionally, the usefulness of the high resolution results generated from the tool to estimate the impact of the defects detected on the operational parameters of the pipeline was emphasised by using the finite element method (FEM), as well as the application of different types of standards defining the durability of defective pipelines such as ASME B31G or RSTRENG.

By repeating inspection runs in the same pipeline, comparative data can be collected for the purpose of estimation of the development rate of the geometry defects as well as the corrosion rate. This study presents some examples of estimating the growth rate of specific defects. It also proposes to adopt the statistical approach for the purpose of the comprehensive assessment of changes occurring in the pipeline as a whole. The applied comparative method allows for identifying zones of significant concentration of defects at an initial stage. Typically, the presence of detected defects is related to the increased activity of the environment onto the pipeline. At the next stage, the method involves analyzing wall loss depth growth rates with statistical and correlation methods. The results of the analysis are then used to forecast the defect growth process and serve as the basis for estimating the period of further safe operation of a pipeline.

CHARACTERISTICS OF MEASUREMENT SYSTEM

In practice, two types of ultrasonic smart pigs are used to probe the pipe walls. Their main purpose is to assess the state of the pipe walls and to detect metal debris and cracks in the material from which the pipes are made. Their idea is to use a set of ultrasonic thickness gauges scanning from inside the surface of the pipe wall. In the case of smart pigs of the first type, the thickness gauges are mounted on a rigid ring and on the other hand on the flexible sleeve. Of course, each of these solutions has its advantages and disadvantages, which we will not analyze here. However, one of the advantages of a rigid ring solution should be pointed. The acoustic beam emitted by the transducer returns to the receiver in form of a series of echoes reflected from the contact surface of materials of different acoustic impedance. The first of these echoes comes from the inner wall surface of the pipeline. Based on the knowledge of the velocity of the sound in the pumped medium, the knowledge of the rigid ring dimensions and on the basis of the measurement of the return time of the first echo it is possible to accurately assess the shape and dimensions of the cross-section of the pipeline. Further echoes come from the reflection of the acoustic beam from the outer surface of the pipe wall. Knowing the sound velocity in the material from which the pipe walls were made and knowing the time intervals between successive echoes, one can accurately determine the wall thickness of the pipeline at the probing site.

Developed and used by us smart pigs are characterized by mounting sensors on a rigid cylinder-shaped ring. With this solution, a series of two measurements reflecting the distance from the face of a sensor from the inner surface of the analyzed pipeline (a stand-off – SO) and the wall thickness (WT) at the point of measurement can be taken with every UT pulse. The pipelines diameter can be determined by measuring two stand-offs mutually shifted by 180° angle, as illustrated in the Fig. 1. Taking into account the measurement resolution in depth of 0.2/0.1 mm and measurement density of approximately 6 mm circumferentially and 3 mm axially, any detected geometry defects can be reflected with high precision. Furthermore, results from particular sensors, imagined as C-scan maps, allow for precise assessment of the size of a defect and determining its impact on the local durability of the pipeline.

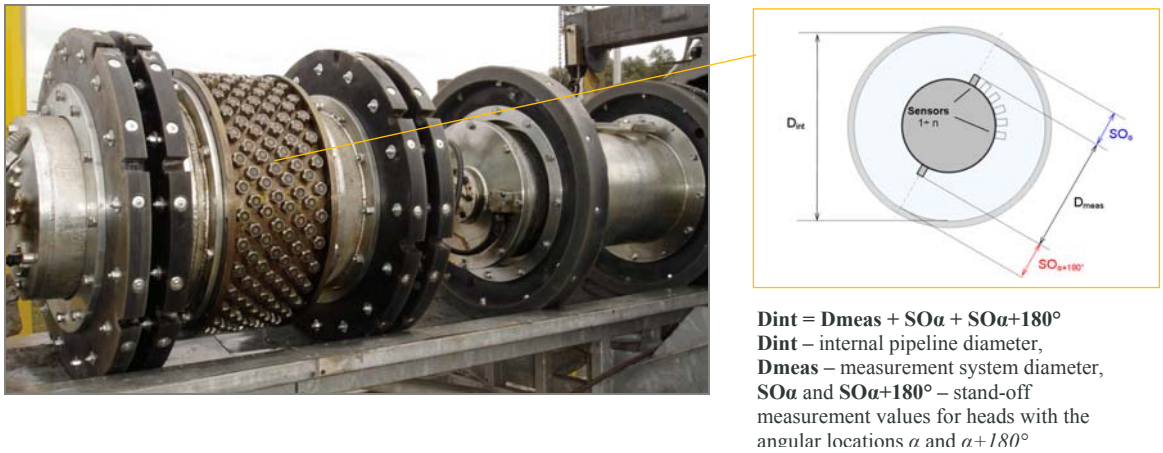

Dint = Dmeas + SOα + SOα+180°
Dint – internal pipeline diameter,
Dmeas – measurement system diameter,
SOα and **SOα+180°** – stand-off measurement values for heads with the angular locations α and $\alpha+180°$

Fig. 1. Example of the smart ultrasound pig measurement principle

Typically, changes in the pipe cross-section geometry are caused as a result of environmental impacts as well as they may be caused by interference of third parties or flaws made during the construction of a pipeline.

A standard case detected during an inspection is a dent caused by a stone. See Fig. 2. The profile of the surface where the stone and pipeline touch causes significant deformations of the pipe wall which may be as deep as 45 mm. A defect of such type puts a pipeline at risk for a number of reasons. First, by deforming a pipeline wall, it causes some stresses which pose a threat to integrity of the pipeline structure. Second, it causes damage and loosening of the insulation which may lead to water accumulation and emergence of a corrosion trap. To assess the impact of the dent on the pipelines operational security, the absolute size of this dent – its depth – must be identified as well as the estimated steepness of the dent walls to be determined on the basis of the recorded measurement data [1,3].

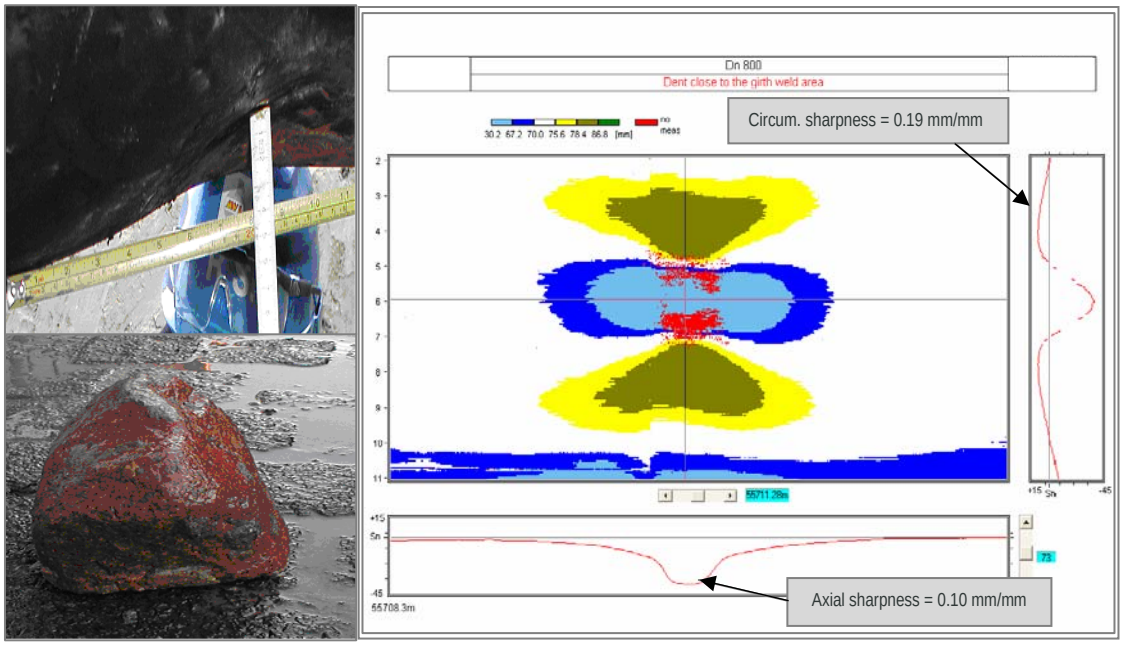

Fig. 2. Dent of a pipeline caused by a stone and a B-scan and C-scan map imagining the wall deformation

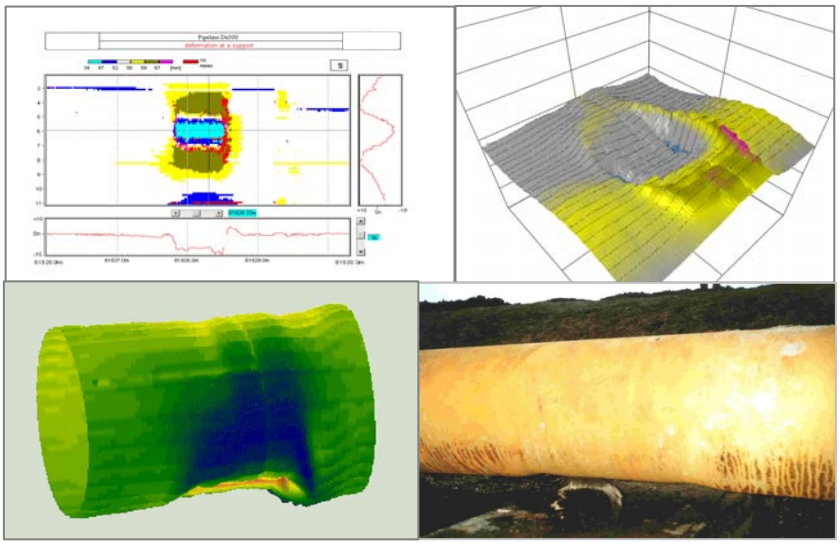

Fig. 3. Dent of a pipeline on a support

Another example of a deformation, shown in Fig. 3, is a pipeline dent caused by a fixed concrete support. Although the contact surface of the support and the pipeline is considerable (0.75 m axially and 0.25 m circumferentially), the average depth of a dent axially reached 13 mm to 15 mm. According to the calculations, stresses within the deformation, in similarity to the above described case, came dangerously close to the yield point of the material, necessitating repair of these pipeline sections [2,3].

By using ultrasonic technology one can also detect mounting errors committed by pipeline builders. The inappropriate spiral joint of adjacent pipes is a frequent structural defect in pipelines. These are cases of reciprocal displacement of axes of adjacent pipes and set-offs resulting from pipe end deformation from the circular cross-section. Such spots are particularly dangerous due to the concentration of tensions in the pipeline structure. Figure 4 shows example of such spots recorded during inspections.

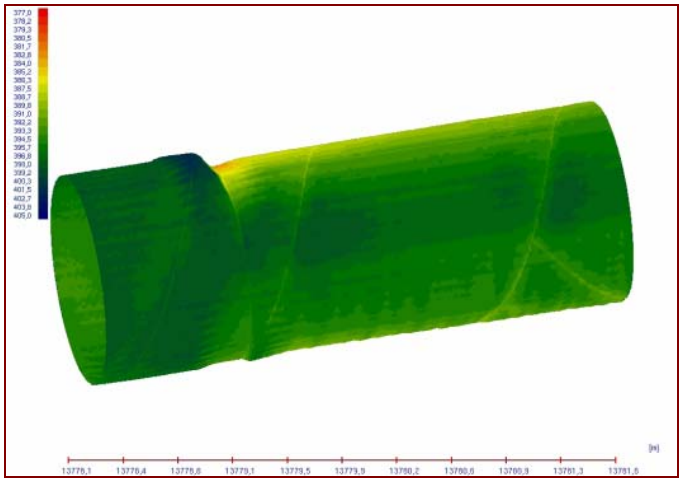

Fig. 4. Examples of axially misaligned adjacent pipes with a set-off on a girth weld

Ultrasonic testing is the oldest and most comprehensive measurement technique of the pipeline wall condition. It allows detection and determination of geometrical parameters of metal losses and material anomalies in the studied structure. After a slight modification, using so-called the skewed heads allow the cracks to be detected in the test material. The biggest

disadvantage is the limitation of the applicability to liquid media. Sometimes it is also used in gas, but it requires technologically difficult inspection in the water stop. The ultrasonic technique is characterized by high precision of measurement and a relatively simple interpretation of the images obtained, due to the direct measurement of the defect geometry as opposed to the magnetic technique in which the geometry of the defects is indirect.

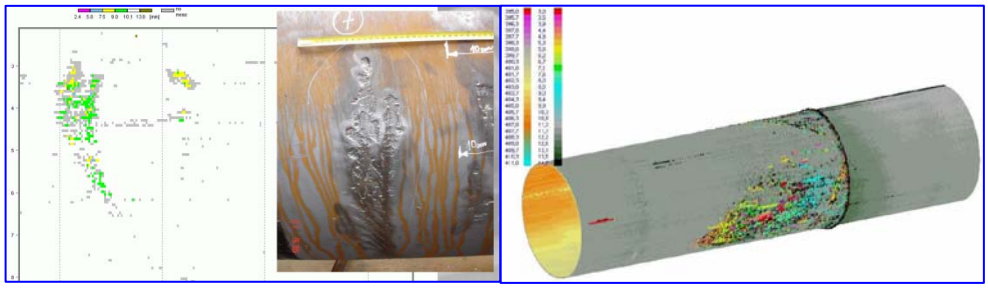

Fig. 5. Examples of anomaly: left outer metal defect, right lamination at the peripheral weld

The detection capabilities of modern UT smart pigs allow detecting and determining the parameters of practically all defects that seriously threaten the safety of the pipeline. Examples of defect detection and various ways of presenting them are shown in Fig. 5.

High resolution smart pigs offer longitudinal resolution of 1-2 mm and circumferential resolution of 5-8 mm. This gives 10-20 measurements per square centimeter of the pipe surface analyzed. With this resolution, the presence of metal debris in the welds can be detected, which using standard pigs is impossible due to the number of failed measurements within the weld resulting from the heterogeneity and due to the uneven surface of the material. An example of the metal loss in the weld is shown in Fig. 6.

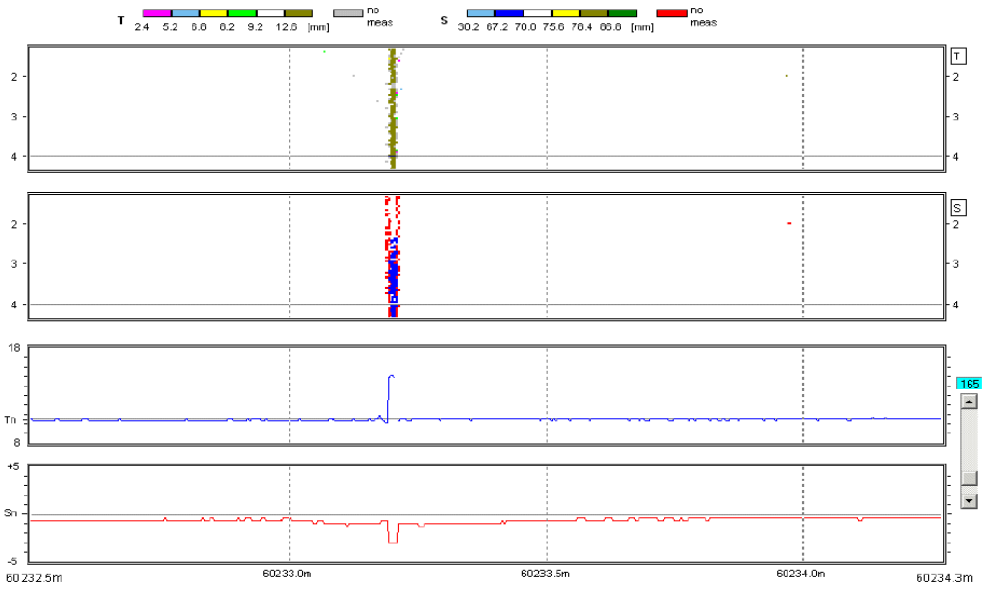

Fig. 6. Material losses within the girth weld

Smart pigs, especially high-resolution ones offer the ability to track the dynamics of defects development. Observation of the development of the defect recorded during subsequent inspections carried out at intervals of several years allows to assess the activity of the defect and to estimate the pace of its development. This is a valuable tip for the operator to schedule a pipeline repairs.

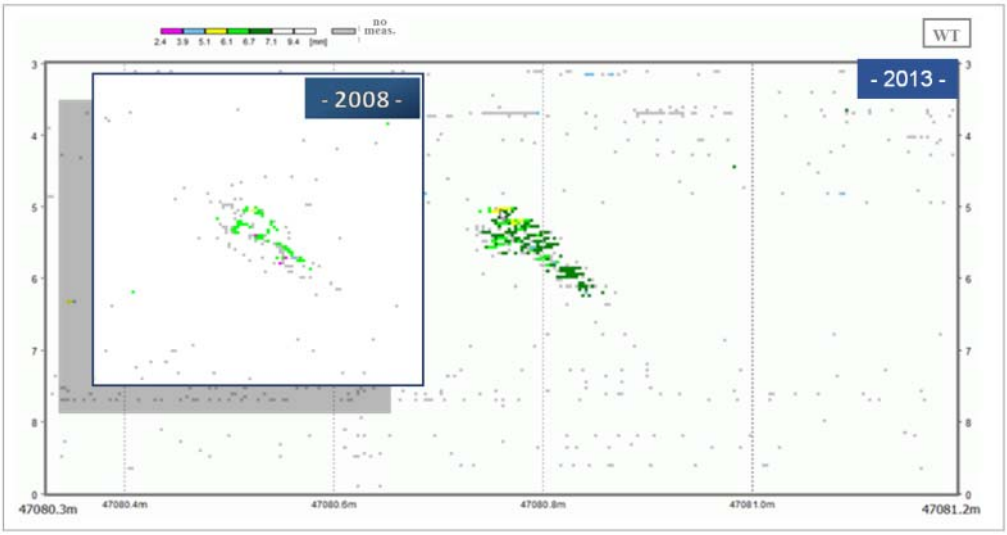

Fig. 7. External Metal Loss – Depth 2008: 1.8/7.8 mm - Depth 2013: 2.4/7.8 mm (L x W = 123 x 206 mm)

Examples of a set of defects images obtained during subsequent inspections at an interval of 5 years are shown in Fig. 7 and Fig. 8. In both cases, C-scan images of the defects show changes which occurred in the damages within a 5-year interval. Fig. 7 shows an external loss of material, its size 123 mm x 206 mm and the depth of 2.4 mm. In 5 years, the depth of the loss grew by 0.6 mm. The defect presented in Fig. 8 is also an external loss of metal but, in this case, it exemplifies a dispersed defect. The defect occurred at the point of contact with a structural element on which the pipeline is suspended. According to the measurement data, the size of the defect is 239 mm x 893 mm and the maximum depth of the loss is 2.6 mm. In a 5-year period, the loss depth growth for the defect is 0.6 mm [4,5,8].

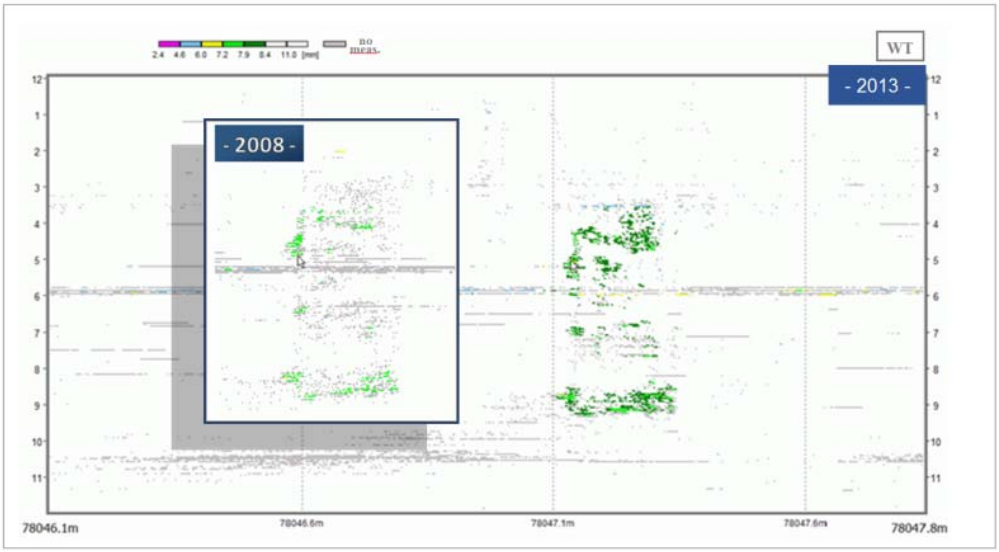

Fig. 8. External Metal Loss – Depth 2008: 2.0/9.0 mm - Depth 2013: 2.6/9.0m m (L x W = 239 x 893 mm)

ANALYSIS OF INSPECTION DATA

The inspection data displayed on the computer screen is subject to assessment and classification by an expert. The data analysis goes on twofold. As a result, two report documents are created. The Pipeline Tally and the Book of Defects and Anomalies. The basic element of the Pipeline Tally is a tabular overview of all pipes and fittings that comprise the pipeline. Each element is described using a set of characteristic parameters (Fig. 9.). For pipes, they are a type of pipe (e.g. longitudinal or spiral welded or seamless), length, average wall thickness, circumferential position of the longitudinal joint, degree of ovality, position on the pipeline route, and for smart pigs equipped with IMUs (Inertial Measurement Unit) also geographical coordinates. Analytical data is complemented by synthetic charts and charts providing comprehensive information on pipeline construction. In the Defects and Anomalies Book, the operator receives a list of all detected defects along with their parametric description. The notion of defect is an object whose parameters exceed in any way the reporting threshold. This threshold, agreed with the contractor, applies to geometric parameters of defects of various types, such as metal loss defects, material defects, defects in geometry, etc. The defects found are subject to classification. International standards and recommendations harmonizing the nomenclature and parameters of individual defects are helpful. The recommendations of the committee working under the guidance of experts such as the Pipeline Operators Forum (POF) recommendations are most often used.

KORSONIC 300 - Pipeline tally of the Begin - End Dn 12", dd.mm.rrrr

	Feature class and localization						Feature parameters								Feature coordinates					Pipe parameter			
															Lambert 72/TAW			WGS84					
Item no	Log distance [m]	Up weld distance [m]	Feature type	Feature identification	Anomaly Dimension class	In class feature no	Length [mm]	Width [mm]	Circum. position [hh:mm]	Depth (peak) [mm]	Depth (mean) [mm]	Reference thickness [mm]	Surface location	ERF	X	Y	Z	Easting	Northing	Length [m]	Weld type	Weld circum. pos. [hh:mm]	Average wall thick. [mm]
1	2	3	4	5	6	7	8	9	10	11	12	13	14	15	16	17	18	19	20	21	22	23	24
1	-3,41	-	WELD		-	1	-	-	-	-	-	-	-	-	161115,33	219557,16	13,42	4°31'41,0783"	51°17'08,7587"	0,35	O	-	22,8
2	-3,06	-	WELD	CHDI, CHWT	-	2	-	-	-	-	-	-	-	-	161115,00	219557,06	13,38	4°31'41,0612"	51°17'08,7553"	2,48	N	-	12,8
3	-1,83	1,23	OFFT																				
5	-0,78	2,28	TEE																				
4	-0,78	2,28	OTHE																				
6	-0,58	-	WELD																				
7	-0,42	-	WELD	C... C...																			
8	0,00	0,42	VALV																				
9	0,42	-	WELD	C... C...																			

KORSONIC 300 - Pipeline tally of the Begin - End Dn 12", dd.mm.rrrr

...on		Feature parameters								Feature coordinates					Pipe parameters						
										Lambert 72/TAW			WGS84								
Anomaly Dimension class	In class feature no	Length [mm]	Width [mm]	Circum. position [hh:mm]	Depth (peak) [mm]	Depth (mean) [mm]	Reference thickness [mm]	Surface location	ERF	X	Y	Z	Easting	Northing	Length [m]	Weld type	Weld circum. pos. [hh:mm]	Average wall thick. [mm]	Internal dia. [mm]	Ovality (×100)	Comment
6	7	8	9	10	11	12	13	14	15	16	17	18	19	20	21	22	23	24	25	26	27
-	1	-	-	-	-	-	-	-	-	161115,33	219557,16	13,42	4°31'41,0783"	51°17'08,7587"	0,35	O	-	22,8	371,1	0,0	*cone*
-	2	-	-	-	-	-	-	-	-	161115,00	219557,06	13,38	4°31'41,0612"	51°17'08,7553"	2,48	N	-	12,8	298,8	0,9	-
-	1	56	55	02:56	-	-	12,8	-	-	161113,83	219556,69	13,21	4°31'41,0012"	51°17'08,7435"	-	-	-	-	-	-	-
-	1	115	113	06:03	-	-	12,7	-	-	161112,84	219556,39	13,07	4°31'40,9497"	51°17'08,7338"	-	-	-	-	-	-	-
-	1	28	25	12:00	-	-	12,7	-	-	161112,84	219556,39	13,07	4°31'40,9497"	51°17'08,7338"	-	-	-	-	-	-	*passage flag*
-	3	-	-	-	-	-	-	-	-	161112,65	219556,33	13,04	4°31'40,9399"	51°17'08,7319"	0,16	F	-	12,9	298,3	0,0	-
-	4	-	-	-	-	-	-	-	-	161112,50	219556,28	13,02	4°31'40,9321"	51°17'08,7304"	0,84	V	-	38,8	304,8	1,2	-
-	1	341	-	01:41	-	-	38,8	-	-	161112,10	219556,16	12,97	4°31'40,9115"	51°17'08,7265"	-	-	-	-	-	-	-
-	5	-	-	-	-	-	-	-	-	161111,70	219556,04	12,92	4°31'40,8909"	51°17'08,7226"	0,16	F	-	12,9	298,3	0,0	-

Fig. 9. Pipeline Tally main table layout

Table sets of pipeline construction elements in the Pipeline Tally complement the statistical charts and graphs showing the length and thickness of the pipes used for the piping, the circumferential position of the longitudinal welds, the average ovality of the individual tubes and the internal diameters of the individual pipes (Fig. 10).

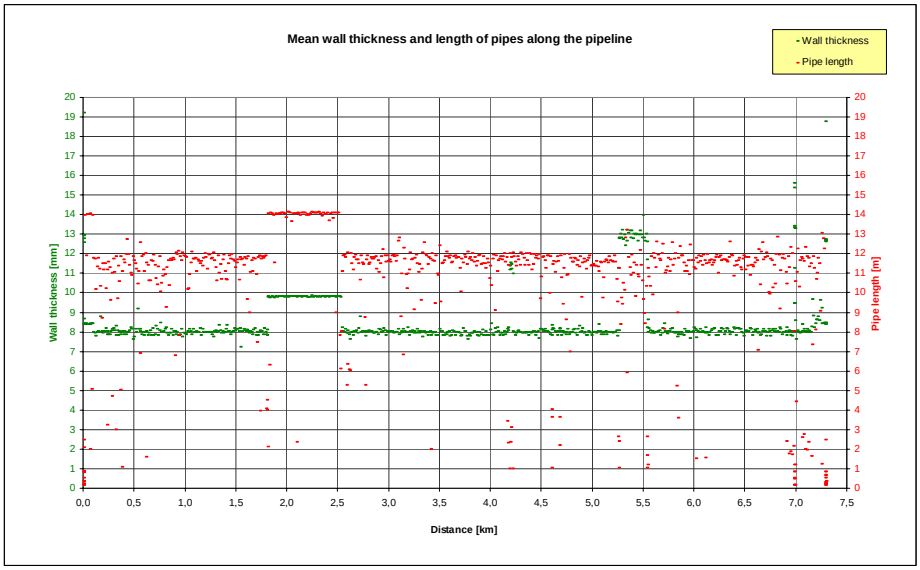

Fig. 10. Pipeline Tally statistics example

Parameters of detected defects include classification of e.g. metal loss defects, lamination, inclusions, dents, etc.; their position along the pipeline and circumferential position, as well as the connection to the Pipeline Tally indicating the tube with the detected defect; geometrical dimensions - length, width and depth. The most important drawbacks are shown in the color maps in B and C (Fig. 11). For metal loss defects, a maximum allowable operating pressure (MAOP) analysis according to certain standards e.g. ASME B31G, RSTRENG or DNV is carried out. For defects of this type, the Estimated Repair Factor is created. The Book of Defects and Anomalies is supplemented by statistical summaries and histograms.

In order to make it easier for the operator to find detected and indicated defects, the report contains synthetic information about defect parameters and their location. An example of such a statement in the form of a defect card is given in Fig. 12. In addition to the complete description of the defect detected, its parameters and color maps, the defect card provides information to facilitate field fault location such as geodetic coordinates, reference to nearest AGMs, and characteristics of neighboring pipes [3,4,5,6].

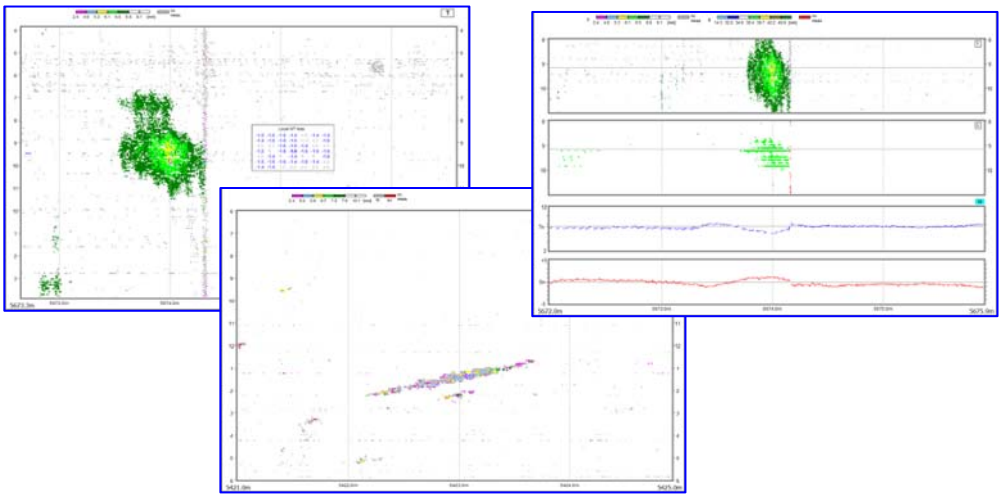

Fig. 11. Examples of color maps (C-scan) for metal defects

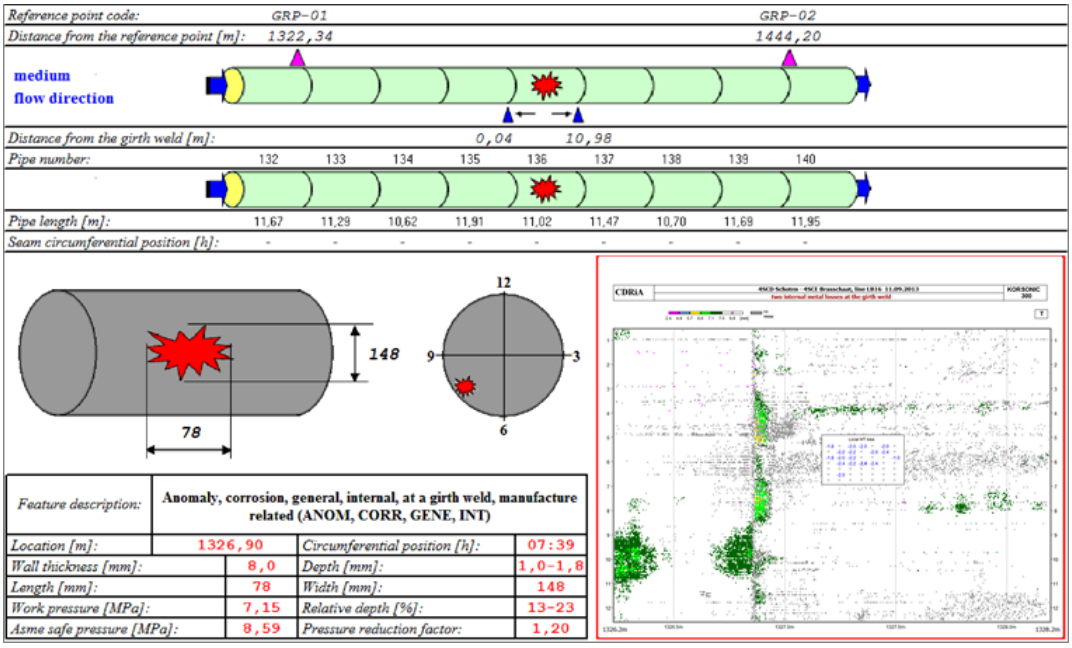

Fig. 12. Defect card example

The Book of Defects and Anomalies is supplemented, according to the POF recommendations, with statistical reports of defects detected in the form of graphs, histograms with respect to depths of defects, intervals of factors influencing operational parameters of the pipeline such as ERF (Estimated Repair Factor) and division of pipelines into sections with their characteristics (Fig. 13).

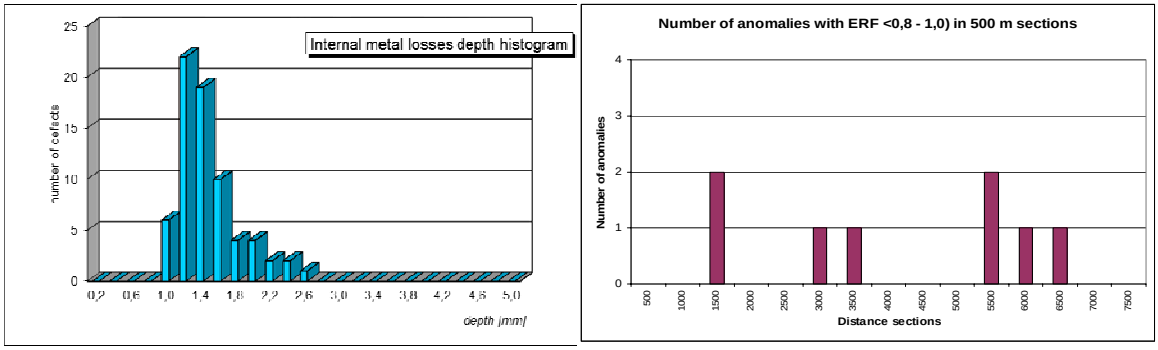

Fig. 13. Book of Defects and Anomalies statistics example

The pipeline operator is pending the inspection of the research smart pig with answers to two questions. Firstly, what are the defects occurring on the studied section and what are the risks for the operation of the pipeline examined? Secondly, to precisely locate them to facilitate and minimize the cost of corrective procedures. Because most of the pipelines are covered with a layer of ground, this requires the use of special navigational techniques that allow precise positioning of the pig throughout its inspection journey. This in turn enables one to determine the coordinates of the detected defects, anomalies, and pipeline infrastructure components. Transformation of obtained navigational information into commonly used geographic or geodetic coordinates enables the integration of pipeline inspection results with

GIS (Geographic Information System) systems, providing a comprehensive database of information on the flow and operating status of the pipeline.

The basic element of the navigation system is the so-called inertial navigation module (IMU), which consists of triad of orthogonal acceleration sensors and triad of orthogonal angular velocity transducers. The sensor set supplements the electronics that control the operation of the sensors and corrects some of the measurement errors caused by, for example, temperature changes. On the basis of recorded measurement data, the trajectory of motion of the device, i.e. the values of the x, y and z coordinates, is determined from the position of the device at successive times. These coordinates are then converted to a user-defined reference system such as WGS84 (GPS compatible) or a selected flat geodetic coordinate system, e.g. UTM, and the height of the point relative to the selected reference level, e.g. Kronstadt.

There are two approaches to determining the trajectory of motion based on IMU measurements. The first is to determine the trajectory based on the dual integration of the accelerometer signal by adjusting the acceleration based on information about the change of spatial orientation derived from gyros. In the second approach, navigation counting uses signals from accelerometers and gyroscopes to track the spatial orientation and corrections of the distance traveled by the odometer system (Fig. 14) [5,6].

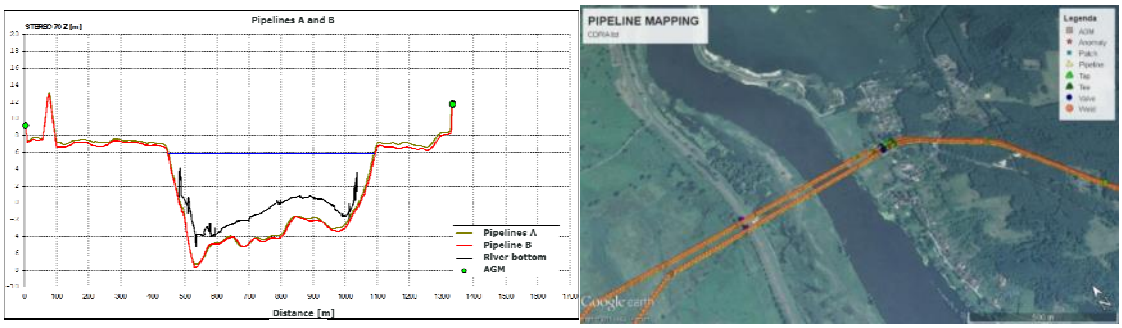

Fig. 14. Examples of the results of using inertial navigation to determine pipeline trajectories under a river bed

Inertial navigation, regardless of the calculation technique used, is associated with the problem of error accumulation. It results in random interferences overlapping with measurements. In the case of accelerometers, these are acceleration resulting from vehicle vibration and the noise of the measuring transducers, while in the case of gyroscopes accidental drift of angular velocity indications.

Despite the use of sophisticated correction techniques such as Kalman filtering, the absolute error increases as you move away from a point with known coordinates. To maintain the measurement error within acceptable limits, the base shortening technique is based on the use of additional correction points with known coordinates obtained, for example, by means of a GPS satellite navigation system. It only remains to associate the results of navigation carried out by smart pig inside the grounded pipeline with the results of GPS measurements performed on its surface. This is most often done with the use of intermediate variable - time.

By synchronizing the clocks of the measurement smart pig and the above ground smart pig transverse detection system under the correction point, we can associate inertial and satellite navigation data and make corrections. Of course, the correction of the pipeline recess under the correction point should be included in the correction. Now it remains only to solve the problem of accurately determining the time of the pig traverse under the correction point. Because the pig moving in the buried pipeline is invisible, noise-sensitive acoustic detectors

generated by the moving pig and electromagnetic wave detectors generated by the specially-designed transmitter on board of the pig are used for this purpose (Fig. 15).

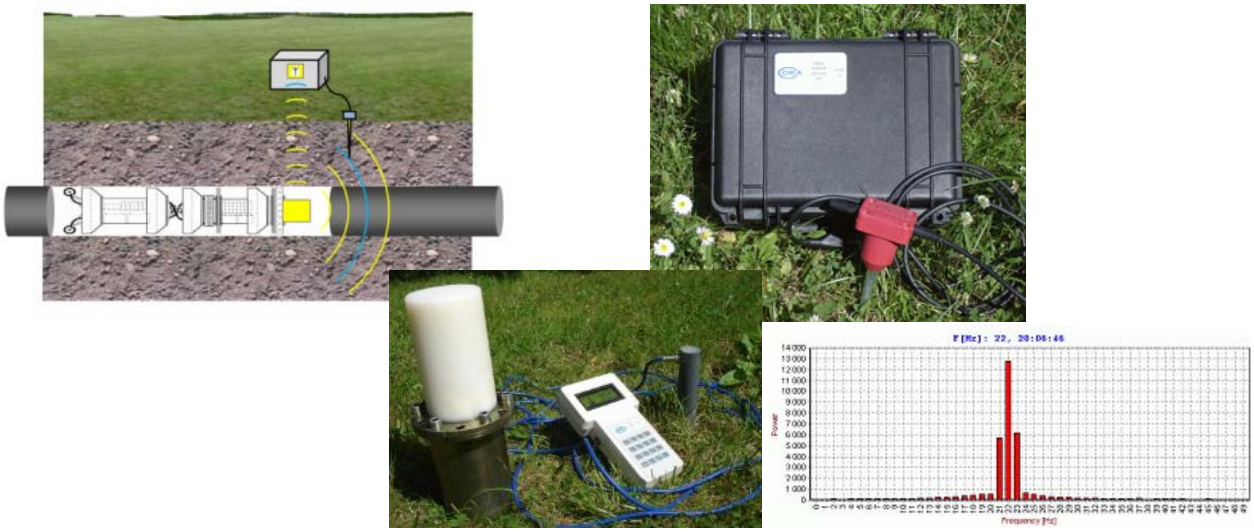

Fig. 15. Detection and timing system of the pig traverse under the AGM

As the mentioned above transducer errors rise over time, the absolute value of the error depends on the travel speed of the smart pig and on the density of the correction points. With existing IMU systems to maintain a navigation error of less than 1 m, it is necessary to move the inspection tool at a speed of 1-3 m/s and use correction points spaced at least 2 km.

ASSESSMENT OF PIPELINE DEGRADATION RATE

As indicated in this title, this chapter discusses the method for analyzing and researching the process of corrosive damages occurring in a pipeline during its operation. The research is based on the measurement results generated during two consecutive inspections.

Analysis of changes occurring in a set of corrosive defects between inspections generates many important data which broaden the current status of knowledge about the pipeline. Results from a single inspection give reflect the current condition of the pipeline at a given moment in time. A comparative analysis of results from two inspections is used to determine the defect growth rate. The data serve as the basis for forecasting the period of future safe operation of the pipeline.

The safe operation period is estimated in accordance with the principles of statistics, with appropriate tolerance range based on the assumed level of confidence. Furthermore, the method enables to identify of single defects which may be the largest or the most likely future obstacles to safe operation of the pipeline.

There are several stages in the proposed method of the analysis, focused on the following issues:

1. analysis of intensity of defect occurrence along the inspected pipeline and identification of the highest defect concentration zones,
2. comparison the measurement data from two inspections,
3. analysis of a schematic growth rate speed profile for defects occurring along the pipeline with identified corrosion activity zones,

4. forecast of the future development of damages and estimating the period of safe operation of the pipeline.

Before starting the analysis, the input defects data must be presented together in a comparative table. Each line of the table is assigned to one specific defect and contains defect-describing parameters which have been measured during the previous and current inspection. Defects from both inspections must be clearly identified and correlated. This principle does not apply to newly developed defects as, in their case, a potential an earlier metal loss in the same spot must be clearly excluded. In this case, a zero loss depth (d=0 mm) is recorded for a defect of the previous period. For the above-mentioned reasons, typically, the source data from inspection is used for preparing the input data.

To facilitate description of the method presented in the paper, each component of the analysis is illustrated with real-life inspection data. The data was collected during the inspection of a sample DN 630 mm pipeline section of 82 km long and the nominal wall thickness of 8 mm. Both inspections were conducted with a 5-year interval (2008 and 2013).

The comparative table is first used to analyze the intensity of defect occurrence along the analyzed pipeline. The number of defects occurring in each running kilometer of the pipeline has been used to measure the intensity. The result of the operation shows that the distribution of defects along the pipeline varies strongly. For more than 80% of the length of the pipeline, defects occur relatively rarely, approximately 1 defect per a section of 2 km. In the remaining part of the pipeline, defects are grouped in the zones of increased concentration. These zones are related to the environment having specific features e.g. industrial infrastructure such as HV lines, railway trucks, industrial facilities or neighborhood of rivers, marshes, etc.

In the zones characterized by higher concentration of defects, their occurrence intensity is many times higher and, in the maximum case, reaches approximately 100 defects/km. In the analyzed pipeline, 7 zones of enhanced corrosive activity were identified. They are marked with symbols S1 ÷ S7. S8 symbol refers to the pipelines sections outside the zones mentioned above. Distribution of the zones is presented in an outline on Fig. 16. Table 1 shows the detailed numeric data.

Table 1.

Marking of the zone	Initial location of the zone [km]	Length of the zone [km]	2008		2013		Growth in the number of defects
			Defects (number)	defect/km	Defects (number)	defect/km	
1	2	3	4	5	6	7	8
S1	16.65	3.01	31	10.3	43	14.3	12
S2	23.06	0.9	13	14.4	16	17.8	3
S3	39.13	1.09	76	69.7	93	85.3	17
S4	43.61	2.31	30	13.0	36	15.6	6
S5	56.86	2.59	51	19.7	82	31.7	31
S6	62.87	1.71	18	10.5	35	20.5	17
S7	76.36	2.63	26	9.9	29	11.0	3
S8	-	68.07	36	0.53	45	0.66	9
Total		**82.3**	**281**		**379**		**98**

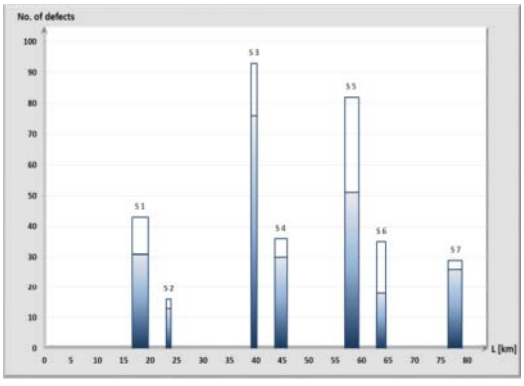

Fig. 16. Distribution of zones demonstrating the highest corrosive activity. The shaded field presents the number of defects found during the previous inspection

The distribution analysis clearly shows that the defect development process occurring in the pipeline is not uniform along the entire length of the pipeline. It also implies that the analysis of the defect development process, covering the entire population of defects, will be of limited use. For this reason, as a rule, it was been assumed that the defect development process is analyzed separately for each detected zone.

The key element of the analysis is the comparison of measurement data from two inspections. As recommended above, the comparative analysis of the measurement data is performed separately for each zone. Zone S3 is selected as illustration of the principle of comparison. According the data on Fig. 16 and Table 1, this part of the pipeline seems the most vulnerable due to the highest density of defect occurrence and significant increase in the number of defects in the 5-year period. The defect growth analysis is based on the correlation table, according to the scheme shown on Fig. 16. The correlation table is a synthetic imaging of the changes which occurred in the set of 93 defects between two consecutive inspections. In the first row of the table, there are three 0 depth defects reported in 2008 and three defects of 1.4, 1.6 and 2.4 mm of depth, identified in 2013 inspection. Defects listed in next rows of the table should have similar interpretation. To facilitate interpretation of the correlation results, the following color scale/coding was used in the table:

- blue background is used for the defects with unchanged depth or demonstrating a difference in their depth of not more than ± 0.2 mm, which corresponds to the measurement resolution of KORSONIC tool,
- beige background is used to highlight defects with their depth growing by 0.4 mm or more,
- white background is used to set off defects with negative growth of depth; physically, negative growth is not possible and only results from comparing two measurements with random uncertainty.

As described above, the results of the earlier inspections are entered in each row while results of the current inspection are presented in the columns.

		Loss depth acc. to the updated report									
	[mm]	1.2	1.4	1.6	1.8	2.0	2.2	2.4	2.6	2.8	Σ
Loss depth acc. to the earlier report	0.0		1	1				1			3
	0.2										
	0.4										
	0.6			1	1		1				3
	0.8		1		2	1		1			5
	1.0	2		2		1	1				6
	1.2	5	2	3	2	1	3	1			17
	1.4	1	1	2	1	3	2	1			11
	1.6		1	2	3	3	3		1		13
	1.8	1	2		2	2	2	2	1	1	13
	2.0				3	3	3	1	1	1	12
	2.2				1	1	5	1	1		9
	2.4				1						1
	2.6										
	2.8										
	3.0										
N		9	8	11	16	15	20	8	4	2	93
$\Sigma n_i\Delta_i$		-0.4	1.4	5.4	3.8	6.2	10.6	8.0	2.8	1.8	39.6
$\Sigma n_i\Delta_i^2$		0.48	2.76	4.84	5.08	4.76	9.80	11.68	2.16	1.64	43.20

	Division into 3 subgroups of defects			All defects
SUBGROUP	I	II	III	I ÷ III
$F(d_i)$	1.2 ÷ 1.6	1.8 ÷ 2.0	2.2 ÷ 2.8	1.2 ÷ 2.8
N	28	31	34	93
$\Sigma n_i\Delta_i$	6.4	10.0	23.2	39.6
$\Sigma n_i\Delta_i^2$	8.08	9.84	25.28	43.20

Fig. 17. The correlation table presenting the depths of external losses for zone S3 and a rough split into 3 subgroups of defects

Additionally, there are 3 rows in the correlation table: the number of N defects for each depth, $\Sigma n_i\Delta_i$ growth sums and sums of squares. To limit the random impact of measurement uncertainty, we also connect several neighboring columns as shown in the correlation table presented on Fig. 17 in its lower part.

The grouping of the columns divides the analyzed zone into several subgroups. Subgroup 1 includes all defects with depth 1.2 to 1.6 mm, totaling 28. Subgroup 2 consists of 31 defects with depth from 1.8 to 2.0 mm. Other defects ranging from 2.2 to 2.8 mm of depth are included in the subgroup 3.

A specific set of Δ_i growths can be found in each subgroup. The value of each growth is a sum of the actual growth of a loss as well as a random component, based on disruptions and measurement uncertainty. Averaging all values of Δ_i growths, it may be assumed that the impact of the random factor will be strongly reduced. Therefore, the mean value of growths in the subgroup is assumed as the most probable value for the set.

Another essential parameter, occurring in a statistical description, is a standard deviation σ. The parameter reflects the measurement of dispersion of individual variables and affects the final estimation of the mean average of growths. The generalized formula used in the statistics to calculate the mean value is:

$$\overline{\Delta_t} = \overline{\Delta} \pm Z * \frac{\sigma}{\sqrt{N}} \tag{1}$$

$\overline{\Delta_t}$ symbol represents the possible range of changes in the mean value, dependent on σ parameter, N variables and the confidence level on which Z variable is dependent in Student's distribution. When the number of N variables is of the order of 30 and the assumed confidence level is 80%, Z variable is approximately 1.3 (the value of Z variable is available in each statistical tables).

The above shows that, on the basis of the above-presented dependence, the higher the measure of σ dispersion is, the wider the range of probable values is $\overline{\Delta_t}$. Also note that the mean value $\overline{\Delta}$ may strictly correspond to the expected value $\overline{\Delta_t}$, when the number of data in a set is very high or when the standard deviation of the variables is scarcely little when compared to $\overline{\Delta}$.

Only the upper confidence range, reaching from $\overline{\Delta}$ to $\overline{\Delta} + Z * \frac{\sigma}{\sqrt{N}}$, is assumed by definition to continue analyzing depths of defects.

Calculation of annual growths of depths is based on the dependencies:

$$\delta_0 = \frac{\overline{\Delta}}{T} \tag{2}$$

with the assumption of mean growth rates,

$$\delta_{max} = \frac{\left(\overline{\Delta} + Z * \frac{\sigma}{\sqrt{N}}\right)}{T} \tag{3}$$

with the assumption of limit growth rates, when T is the interval between inspections in years.

The statistical analysis shows that calculation of strictly defined value of annual growths should not be expected; however, the analysis allows for calculating the upper and lower limit which contain the most probable value of growth rates. The course of the analysis and calculation of the annual growths in the defect depths for S3 zones are given in Table 2.

Using the same approach to other zones, the defect growth rates for the entire pipeline is calculated. Fig. 18 is a graphic presentation of the results of the calculation as a schematic profile of defect growth rate.

Defect growth rate parameters presented in Fig. 18 show how strong and varied is the environment impact on individual parts of the pipeline. Two zones, S1 and S3, can be

characterized by the highest defect growth activity, contrary to S4 and S7 zones, which show the growth parameter is more than twice smaller.

Table 2. *Calculation of the annual growths of defect depths for S3 zone in 3 subgroups and for the case when division into groups was omitted*

No.	DEFECT SUBGROUP		I	II	III	All defects
1.	Loss depth brackets	[mm]	1.2 ÷ 1.6	1.8 ÷ 2.0	2.2 ÷ 2.8	1.2 ÷ 2.8
2.	Defects (number)	[pcs.]	28	31	34	**93**
3.	The mean value of growths for the entire	[mm]	0.229	0.323	0.682	**0.426**
4.	Standard deviation of growths	[mm]	0.495	0.470	0.535	**0.535**
5.	Range of statistical uncertainty when estimating the mean values of growths 80%	[mm]	0.123	0.110	0.120	**0.072**
6.	Mean annual growth of defect depth	[mm/year]	0.046	0.065	0.136	**0.085**
7.	Annual growth limit of defect depth	[mm/year]	0.070	0.087	0.161	**0.099**

ZONE	Number of defects	Depth range			Ranges of the annual depth growths for individual defect subgroups in the zone [mm/year]
S1	20	1.2	÷	1.8	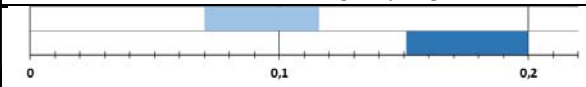
	23	2.0	÷	3.4	
S2	16	1.2	÷	2.8	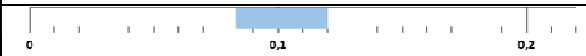
S3	28	1.2	÷	1.6	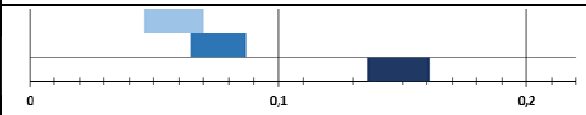
	31	1.8	÷	2.0	
	34	2.2	÷	2.8	
S4	18	1.2	÷	1.6	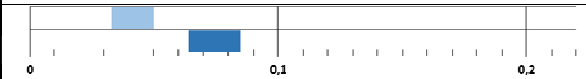
	18	1.8	÷	2.4	
S5	31	1.2	÷	1.4	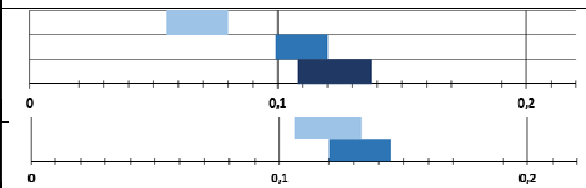
	28	1.6	÷	1.8	
	23	2.0	÷	2.8	
S6	20	1.2	÷	1.6	
	15	1.8	÷	2.6	
S7	29	1.2	÷	2.8	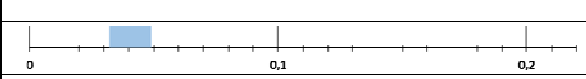
S8	26	1.2	÷	1.6	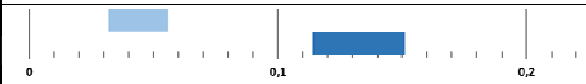
	19	1.8	÷	2.4	

Fig. 18. The growth rate profile of defects along the pipeline per depth range per each zone

Furthermore, the results of the correctly conducted analysis show a regularity occurring in each zone. According to the results, defect growth rate parameters have the highest value when defects are the deepest. On this basis, it is assumed that the defect aggravation process accelerates with depth.

Defect growth rate parameters, in connection with the results of the most recent inspection results, form the basis for forecasting further development of defects. For the purpose of this paper, 3 forecasting periods were assumed: after 5, 7 and 10 years of

operation. Each forecast is based on the top and medium value of the annual defect growth rate, according to the calculations shown in the Table 2 and on the Fig. 18.

The complete result of the forecast is presented in the final report as a multi-page table covering all defects included in the defect and anomaly table in the inspection report. For the purpose of the paper, results of the forecast are limited to the defects which go beyond the safe operational threshold of a pipeline.

Two thresholds were taken into consideration:

- the basic threshold, based on the maximum allowed operating pressure MAOP, calculated in accordance with ASME B31G,
- the additional threshold, representing 50% of the wall thickness in case of dispersed defects.

Table 3 presents the potential process of defect growth in the inspected pipeline, for three forecasting periods.

Table 3. *Forecast of the number of defects beyond the safe operational threshold per defect concentration zone*

TYPE OF FORECAST:	5 year		7 year		10 year	
ZONE	Defect growth rate parameters					
	mean	max.	mean	max.	mean	max.
S1	-	1	1	5	8	15
S2	-	-	-	-	-	6
S3	1	1	1	2	6	25
S4	-	-	-	-	-	-
S5	-	-	-	-	-	4
S6	-	-	-	-	1	3
S7	-	-	-	-	-	-
S8	-	-	-	-	-	3

Forecast results, presented in Table 3 are largely convergent with the defect growth rate parameters shown in Fig. 8. Zones S1 and S3 contain defects which may be first to disrupt safe operational conditions of the pipeline.

On the basis of the data, it is concluded that, with the planned 5-year inspection interval, 1 to 2 defects will require an earlier repair. For comparison: if the inter-inspection interval is extended to 7 years, the number of forecast earlier repairs should be 2 to 7, Extension of the interval to 10 years causes a significant growth of essential defects along the entire pipeline length.

According to the data, the optimal strategy which guarantees safe operation of the inspected pipeline is to assume and plan a 7-year inspection interval combined with a pre-defined number of earlier repairs (2 to 7) [7,8].

SUMMARY

If technical installations are to guarantee operational safety and reliability, they must be systematically controlled. The institutions responsible for the installations in use and the legislator know this. Emerging and increasingly stringent regulatory arrangements are in place that impose specific obligations on device and plant diagnostics. Pipeline operators are pushing the testing companies to make the tests as cheap as possible and as quickly as

possible to minimize interference with the normal operation of the plant. This involves the integration of different measuring and diagnostic techniques into one diagnostic device. Ultrasound techniques play a very important role in this regard. This technique enables the evaluation of a wide range of pipeline parameters with high accuracy and reliability. Special techniques allow the use of ultrasonic technology also for gas pipeline testing. Linking different measurement techniques into one diagnostic device also has the good side that the information provided to the operator after the diagnostic test is more complete, more reliable and less expensive for the operator.

By minimizing costs, inspection companies modify the structures of the used diagnostic tools. Modular constructions in which individual modules perform different measurements or use different measurement techniques are becoming more and more common. The results are mutually synchronized and complement each other. These solutions allow you to respond dynamically to one's needs and to align one's inspection equipment with those modules that will best meet your requirements.

Assessment of the condition of oil pipelines, prepared on the basis of inspection results, is usually a task which requires a lot of time and effort. It is also because of the considerable size of the set of the data contained in the reports. While there are precise methods determining the impact of a defect onto the life of a pipeline, selection of several hundred or more defects in terms of their highest importance for safe operation of a pipeline is a difficult task.

The method involving the comparative analysis of results from two inspections, described in the paper, leads to considerable streamlining of the defect analysis and selection process. The method is based on two main types of analyses.

The first method analyses intensity of defect occurrence along the pipeline, leading to detection of the most corrosion-active zones of the pipeline. Typically, such parts are related to the presence of industrial infrastructure or specific geographic environment.

The purpose of the other analysis is to have a correlation-based comparison of sets of defects from each inspection, separately for each zone. Owing to this approach, detailed distribution of defect growth rate per zone of the pipeline is known. The example discussed in the paper shows that annual defect growths demonstrate considerable differences depending on the location of defect concentration along the pipeline.

The defect development process analysis, described in the paper, may be used for a number of purposes, including:

- preparation of the optimum strategy of the repair program,
- forecasting the safe operation period of a pipeline, depending on the repair plan,
- assessing the effectiveness of pipeline protection measures.

REFERENCES

1. Lubkiewicz J., Raczyński P., Łukajtis W., Diagnozowanie stanu technicznego rurociągów z zastosowaniem tłoków inteligentnych. Nafta & Gaz Biznes 4 (2000), 15-17.
2. Bogotko W., Lubkiewicz J., Raczyński P.,: Przygotowanie rurociągów do inspekcji tłokami inteligentnymi. Nafta & Gaz Biznes 6 (2000), 15-18.
3. Bogotko W., Dąbrowski L., Lubkiewicz J., Raczyński P., Stress assessment in deformed pipelines based on calliper pig surveys. Proc. 4th International Conference on Pipeline Rehabilitation & Maintenance, Prague, Czech Republic, 2000, Paper 3, 1-13.

4. Bogotko W., Raczyński P., Skrok K., Rola tłoków inteligentnych w zapewnieniu niezawodności rurociągów dalekosiężnych. Proc. X Międzynarodowa Konferencja Naukowo-Techniczna Konstrukcje Metalowe, Gdańsk, Poland 2001, Vol. 3, 105-112.
5. Raczyński P., Bogotko W., Leszczyński T., Wykorzystanie ultradźwiękowych tłoków pomiarowych do oceny uszkodzeń korozyjnych ścianek rurociągów magistralnych oraz wpływu ich na parametry eksploatacyjne. Proc. Międzynarodowa Konferencja Nowoczesne Metody Monitorowania Korozji Dla Oceny Strat Korozyjnych i Kosztów Korozji, Jurata, Poland, 2003, 153-161.
6. Raczyński P., Warnke K., Diagnostyka stanu technicznego rurociągów stalowych z wykorzystaniem tłoków ultradźwiękowych wysokiej rozdzielczości. Ochrona przed korozją 8 (2014), 316-319.
7. Raczyński P., Analysis and Trend Estimation of Geometry Defects and Metal Losses in the Pipeline Wall Based on UT Intelligent Pig Inspection. Proc. 9-th Pipeline Technology Conference, Berlin, Germany, (2014) Proceedings on the CD.
8. Raczyński P., Lewandowski M., Method and Tool Used to Predict the Service Life of a Pipeline. Pipeline Operations & Management Conference, Bahrain, 2016.